Nature of the hydrogen bridge in transition metal complexes

IV *. Comparison of the electronic structure of the phosphine- and carbonyl-molybdenum dimers with double hydrogen bridge

Bogusława Jeżowska-Trzebiatowska and Barbara Nissen-Sobocińska

Institute for Low Temperature and Structure Research, Polish Academy of Sciences, Plac Katedralny 1, P.O. Box 937, 50-950 Wrocław (Poland)

(Received December 22nd, 1988)

Abstract

The influence of the terminal ligands on the electronic structure and stability of the hydrogen bond between metal atoms has been characterized on the basis of the molecular orbital calculations by use of the parameter-free Fenske–Hall and EHT methods for phosphine- and carbonyl-molybdenum dimers. The electronic structures of $[(PH_3)_4Mo\langle{}^H_H\rangle Mo(PH_3)_4]^{2+}$ and $H(PH_3)_3Mo\langle{}^H_H\rangle Mo(PH_3)_3H$ are discussed and compared with the electronic structure of $[(CO)_4Mo\langle{}^H_H\rangle Mo(CO)_4]^{2-}$.
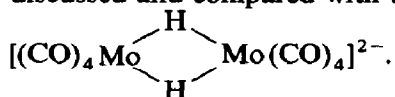
The role played by the *3d* AO's of the phosphorous atoms in the formation of the terminal (PH_3)–Mo bonds is described.

Introduction

In our previous paper [1] we discussed the electronic structure of the carbonyl binuclear molybdenum complex with double hydrogen bridge $[(CO)_4Mo\langle{}^H_H\rangle Mo(CO)_4]^{2-}$. Molybdenum also forms the phosphine dimer with the same bridge viz. $H(PMe_3)_3Mo\langle{}^H_H\rangle Mo(PMe_3)_3H$ [2]. The molecular structure of this complex is interesting in several respects. Phosphine groups are the donors

---

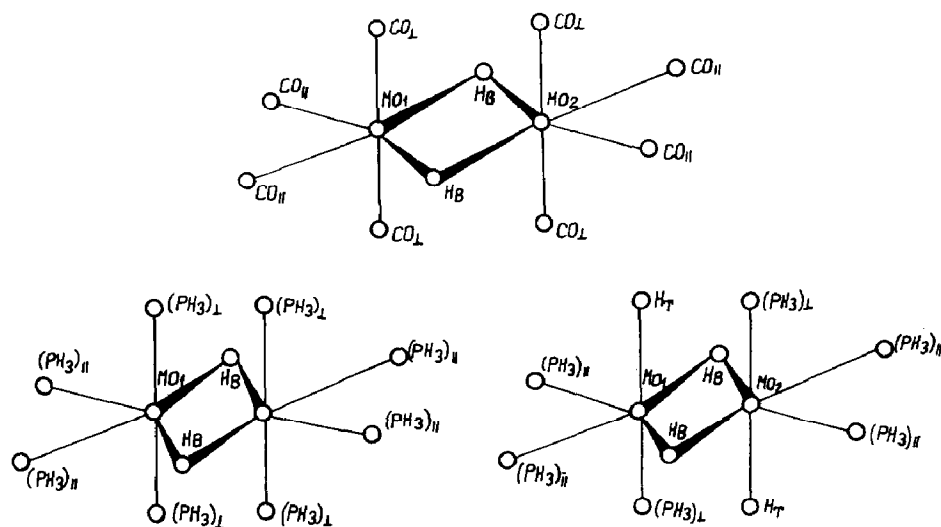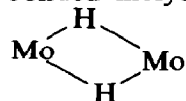Fig. 1. Molecular structure of $[(CO)_4Mo\underset{H}{\overset{H}{\diagdown\diagup}}Mo(CO)_4]^{2-}$, $[(PH_3)_4Mo\underset{H}{\overset{H}{\diagdown\diagup}}Mo(PH_3)_4]^{2+}$ and $H(PH_3)_3Mo\underset{H}{\overset{H}{\diagdown\diagup}}Mo(PH_3)_3H$ as assumed for the calculations.

i.e. they have a different character than the CO groups which are the terminal ligands in the complexes discussed earlier [1,2]. The very short Mo–Mo distance, equal to 2.19Å, is well within the region of values characteristic for the quadruply bonded molybdenum atoms [2]. The asymmetry of the double hydrogen bridge $Mo\underset{H}{\overset{H}{\diagdown\diagup}}Mo$ has been revealed by an X-ray diffraction study [2]. The important feature of this complex is that there are two terminal hydrogen atoms. Thus, we can compare the character and stability of the bridge Mo–H–Mo and terminal Mo–H bonds.
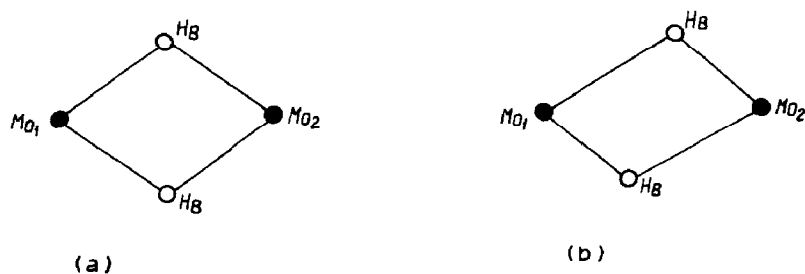

Fig. 2. Symmetric and asymmetric hydrogen bridge core for phosphine dimer of molybdenum: (a) $Mo^1-H^B = Mo^2-H^B = 1.61$ Å, (b) $Mo^1-H_B = 1.61$, $Mo^2-H^B = 1.43$ Å.

We carried out the molecular orbital calculations by means of the parameter-free Fenske–Hall and by empirical EHT methods for $[(PH_3)_4 Mo \overset{H}{\underset{H}{\diamond}} Mo(PH_3)_4]^{2+}$

with symmetric $Mo \overset{H}{\underset{H}{\diamond}} Mo$ and asymmetric $Mo \overset{H}{\underset{H}{\diamond}} Mo$ bridges (Fig. 1) as

well as for $H(PH_3)_3 Mo \overset{H}{\underset{H}{\diamond}} Mo(PH_3)_3 H$ and compared our results with the

electronic structure of $[(CO)_4 Mo \overset{H}{\underset{H}{\diamond}} Mo(CO)_4]^{2-}$ discussed in detail previously (Fig. 2).

The coordinate systems on the atoms assumed for calculations for studied phosphine complexes are presented in Fig. 3. The structural parameters for the calculations were assumed on the basis of the crystallographic structure for $HPMe_3 Mo \overset{H}{\underset{H}{\diamond}} Mo PMe_3 H$ [2]. We have assumed that the $Mo-PH_3$ bonds have the same lengths for the PH_3 groups perpendicular to the bridge plane ($(PH_3)_I$) as the PH_3 groups in the bridge plane ($(PH_3)_{II}$). The bond lengths used by us for the calculations were: $Mo-Mo = 2.19$, $Mo-P_I = Mo-P_{II} = 2.43$, $Mo-H^B = 1.61$ Å for the symmetric bridge and $Mo^1-H^B = 1.43$, $Mo^2-H^B = 1.61$ Å for the asymmetric bridge (H^B = bridge hydrogen atom), $Mo-H^T = 1.82$ Å (H^T = terminal hydrogen atom) and the angles were: $Mo-H^B-Mo = 92$, $P_I-M-P_I = 180$, $P_{II}-M-P_{II} = 90$ and $P_I-M-H^T = 90°$. Suitably optimized functions of the following types: $1s$, $2s$, $2p,\ldots,4d$, $5s$, $5d$ of the Mo atoms, the $1s$, $2s$, $2p$, $3s$, $3p$ of the P atoms, and $1s$ of the H atoms were applied on the calculations carried out by use of the Fenske–Hall method [3]. The atomic valence base for the EHT calculations [4] contained the following functions: $4d$, $5s$, $5p$ for the Mo atoms and $3s$, $3p$, $3d$ for the P atoms and $1s$ for the H atoms.
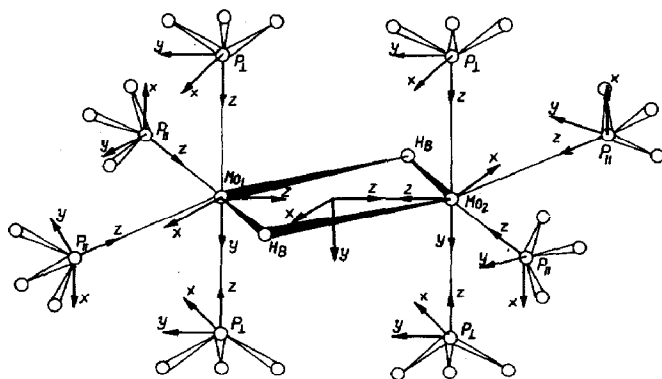

Fig. 3. Coordinate systems assumed in calculations for $[(PH_3)_4 Mo \overset{H}{\underset{H}{\diamond}} Mo(PH_3)_4]^{2+}$.

Results and discussion

The filled energy levels of $[(PH_3)_4Mo{\overset{H}{\underset{H}{<>}}}Mo(PH_3)_4]^{2+}$ with symmetric $Mo{\overset{H}{\underset{H}{<>}}}Mo$ bridge, calculated by use of Fenske–Hall method, can be classed as follows:

(1) from -38.88 to -25.09 eV, levels which correspond to MO's of PH_3 groups or the $PH_3-4d_{x^2-y^2}Mo$ bonding interactions,

(2) -24.85 eV energy level $(3b_{3u})$ of the Mo–H–Mo bridge bond character,

(3) from -24.28 to -23.10 eV, levels which correspond to MO's of PH_3 groups or to $PH_3-4d_{x^2-y^2}$ interactions,

(4) -22.41 and -22.08 eV energy levels $(4b_{3u}$ and $6a_g$ respectively) of the Mo–H–Mo bridge bond character,

(5) -20.85, -20.73 and -20.52 eV energy levels $(5b_{1u}$, $3b_{3g}$ and $4b_{2g}$ respectively), which correspond to $PH_3-4d_{x^2p_y^2}Mo$, PH_3-5p_yMo and $PH_3-4d_{xz}Mo$ bonding interactions,

(6) -19.90 and -19.46 eV levels $(5b_{3u}$ and $7a_g)$ of the Mo–H–Mo bridge bond character,

(7) from -16.59 to -12.51 eV energy levels which correspond mainly to metal-metal interaction $(8a_g, 5b_{2u}, 3b_{1g}, 3a_u)$,

(8) -12.24 eV nonbonding level $(4b_{3g})$ exclusively of $(PH_3)_1$ character,

(9) -11.91 eV HOMO level $(4b_{1g})$ which correspond to PH_3-dMo interaction.

The highest of these levels are presented in Table 1 and in Fig. 4. The group of the lowest unfilled energy levels corresponds mainly to the metal–metal interactions (Table 1). Of the four filled energy levels having mainly metal AO character, only the $8a_g$ and $5b_{2u}$ levels provide the bonding contributions to the direct metal–metal bond. The $8a_g$ level corresponds to the $\sigma d-\sigma d$ bonding interaction and $5b_{2u}$ corresponds to the $d\pi-d\pi$ bonding interactions. But the $\delta d-\delta d$ bonding level $(3b_{1g})$ corresponds to the $\delta d-\delta d$ antibonding level $(3a_u)$. Thus these two levels do not contribute to the direct metal–metal bond (Fig. 5). Taking into account that bridge energy level $3b_{3u}$(43% $4d_{xz}Mo$) also corresponds to M–M bonding interaction we can roughly assume that M–M bond order is only slightly greater than two (in spite of the short distance between metal atoms, suggesting quadruply bonded metal atoms [2]). The occurence of a large direct bonding interaction between the metal atoms in $[(PH_3)_4Mo{\overset{H}{\underset{H}{<>}}}Mo(PH_3)_4]^{2+}$ also appears in the M–M overlap population of 0.200 (Table 2). It is noteworthy that in the carbonyl dimer $[(CO)_4Mo{\overset{H}{\underset{H}{<>}}}Mo(CO)_4]^{2-}$ the bonding interaction between the metal atoms is exclusively through the double hydrogen bridge, which results in the M–M overlap population that is close to zero [2].

Last two filled energy levels in $[(PH_3)_4Mo{\overset{H}{\underset{H}{<>}}}Mo(PH_3)_4]^{2+}$ $(4b_{3g}, 4b_{1g})$ have mainly the character of phosphine groups which are perpendicular to bridge plane

Table 1

Energies and compositions of the highest occupied molecular energy levels of $[(PH_3)_4Mo\diagdown\!\!{}^H_H\!\!\diagup Mo(PH_3)_4]^{2+}$ with symmetric double hydrogen bridge and D_{2h} symmetry calculated by use of the Fenske–Hall method

MO	Energy (eV)	Greatest contributions by valence atomic orbitals (%)									
$5b_{2g}$	−5.22	$4d_{xz}$Mo	57	$5d_{xz}$Mo	15	sH$_I$	12	p_yP$_{II}$	9		
$5b_{3g}$	−8.20	$4d_{yz}$Mo	88	$5d_{yz}$Mo	3	p_zP	3	sH$_I$	2		
$6b_{1u}$ LUMO	−11.28	$4d_{z^2}$Mo	39	$4d_{x^2-y^2}$Mo	25	p_zMo	13	sH$_I$	13	p_yP$_{II}$	12
$4b_{1g}$ HOMO	−11.91	sH$_I$	44	$4d_{xy}$Mo	17	p_yP$_I$	13	$4d_{z^2}$Mo	10		
$4b_{3g}$	−12.24	sH$_I$	64	p_yP$_I$	16	sP$_I$	8	p_xP$_I$	6		
$3a_u$	−12.51	$4d_{xy}$Mo	94	sH$_I$	3						
$3b_{1g}$	−14.16	$4d_{xy}$Mo	77	sH$_I$	12	p_xP$_I$	4	p_yP$_I$	2		
$5b_{2u}$	−15.83	$4d_{yz}$Mo	96	sH$_I$	1						
$8a_g$	−16.59	$4d_{z^2}$Mo	72	$4d_{x^2-y^2}$Mo	15	sH^B	5	p_zP$_{II}$	2		
$7a_g$	−19.48	sH^B	25	p_zP$_{II}$	19	p_yP$_{II}$	16	p_zMo	13		
$5b_{3u}$	−19.90	p_yP$_{II}$	30	p_zP$_{II}$	29	sH^B	14	sP$_{II}$	12		
$4b_{2g}$	−20.52	p_yP$_{II}$	43	p_zP$_{II}$	22	sH$_{II}$	12	$4d_{xz}$Mo	10		
$3b_{3g}$	−20.73	p_zP$_I$	60	p_yMo	18	sP$_I$	11	sH$_I$	8		
$5b_{1u}$	−20.85	p_yP$_{II}$	32	p_zP$_{II}$	25	sP$_{II}$	15	sP$_{II}$	10		
$6a_g$	−22.08	sH$_I$	40	p_yP$_{II}$	24	sH$_{II}$	11	$4d_{x^2-y^2}$Mo	9		
$4b_{3u}$	−22.41	sH$_{II}$	38	p_yP$_{II}$	28	sH^B	14	sH^B	11		
$3b_{2g}$	−23.10	sH$_{II}$	36	p_zP$_{II}$	32	p_yP$_{II}$	16	sP$_{II}$	5		
$4b_{1u}$	−23.18	p_zP$_I$	42	$4d_{x^2-y^2}$Mo	11	sH$_{II}$	11	p_zP$_{II}$	10		
$3b_{1u}$	−23.59	p_zP$_{II}$	32	sH$_{II}$	31	p_yP$_{II}$	18	p_zP$_{II}$	7		
$5a_g$	−23.79	p_zP$_{II}$	31	sH$_{II}$	31	p_yP$_{II}$	19	sH^B	5		
$4b_{2u}$	−24.28	p_zP$_I$	54	sH$_I$	16	sP$_I$	11	p_xP	11		
$3b_{3u}$	−24.85	$4d_{xz}$Mo	43	p_zP$_{II}$	38	p_zP$_{II}$	15	sH$_{II}$	7		
$2a_u$	−25.09	p_xP$_I$	44	p_xP$_I$	47	p_zP$_I$	4	p_yP$_I$	1		

H^B = bridge hydrogen atom, H$_I$ = hydrogen atom of the PH$_3$ group perpendicular to bridge plane, H$_{II}$ = hydrogen atom of PH$_3$ group in bridge plane, P$_I$ = phosphorous atom perpendicular to the bridge plane, P$_{II}$ = phosphorous atom in the bridge plane.
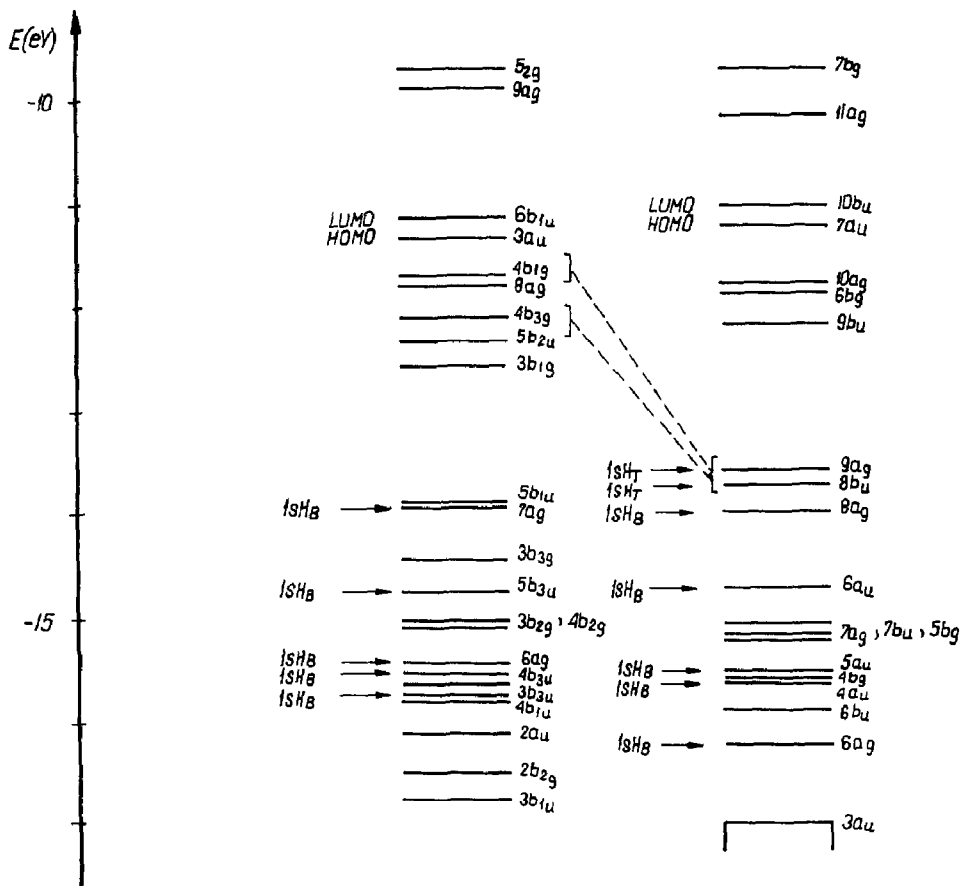
Fig. 4. Correlation of the molecular energy levels of $[(PH_3)_4 Mo\diagdown_H^H\diagup Mo(PH_3)_4]^{2+}$ and $H(PH_3)_3 Mo\diagdown_H^H\diagup Mo(PH_3)_3 H$ calculated by use of Fenske–Hall method.

$((PH_3)_I)$. The replacement of the two $(PH_3)_I$ groups with H^- anions after transition to $H(PH_3)_3 Mo\diagdown_H^H\diagup Mo(PH_3)_3 H$ changes the $4b_{3g}$ and $4b_{1g}$ levels into two $Mo–H^T$ interaction levels, which are in an energy region between the $Mo–H–Mo$
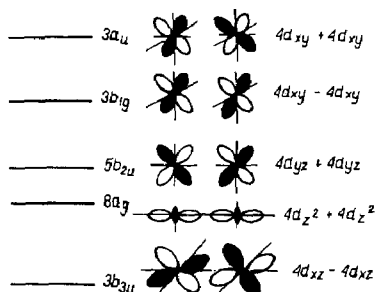

Fig. 5. Filled molecular energy levels corresponding mainly to metal–metal interactions.

Table 2a. Mulliken overlap populations

Compound	Overlap populations				
	M—M	M—H^B	M—L$_I$	M—L$_{II}$	M—H
Calculated by Fenske – Hall method [a]					
$[(PH_3)_4Mo(\mu\text{-}H)_2Mo(PH_3)_4]^{2+}$ (s, a)	0.222	0.157	0.239	0.156	
$[(CO)_4Mo(\mu\text{-}H)_2Mo(CO)_4]^{2-}$ (a)	−0.008	0.118	0.400	0.381	
$[(CO)_4Mo(\mu\text{-}H)_2Mo(CO)_4]^{2-}$ (b) [1]	0.023	0.147	0.418	0.395	
Calculated by EHT method [b]					
$[(PH_3)_4Mo(\mu\text{-}H)_2Mo(PH_3)_4]^{2+}$ (s)	0.301	0.324	0.694	0.616	
$H(PH_3)_3Mo(\mu\text{-}H)_2Mo(PH_3)_3H$ (s)	0.363	0.330	0.751	0.781	0.404
$[(CO)_4Mo(\mu\text{-}H)_2Mo(CO)_4]^{2-}$ [1]	0.066	0.301	0.839	0.839	

L$_I$ = terminal ligand in perpendicular plane to hydrogen bridge, L$_{II}$ = terminal ligand in hydrogen bridge plane, H^B = bridge hydrogen atom, H^T = terminal hydrogen atom, s = symmetric hydrogen bridge, a = calculated with inclusion of 5d AO's of Mo, b = calculated without inclusion of 5 AO's of Mo.
[a] Without inclusion of 3d AO's of P. [b] With inclusion of 3d AO's of P.

Table 2b. Mulliken atomic charges

Compound	Atomic charges				
	M	H^B	L$_I$	L$_{II}$	H^T
Calculated by Fenske-Hall method [a]					
$[(PH_3)_4Mo(\mu\text{-}H)_2Mo(PH_3)_4]^{2+}$ (s, a)	0.374	−0.431	0.304	0.230	
$[(CO)_4Mo(\mu\text{-}H)_2Mo(CO)_4]^{2-}$ (a)	1.243	−0.488	−0.405	−0.474	
$[(CO)_4Mo(\mu\text{-}H)_2Mo(CO)_4]^{2-}$ (b)	0.746	−0.331	−0.316	−0.391	
Calculated by EHT method [b]					
$[(PH_3)_4Mo(\mu\text{-}H)_2Mo(PH_3)_4]^{2+}$ (s)	1.554	−0.223	−0.123	−0.037	
$H(PH_3)_3Mo(\mu\text{-}H)_2Mo(PH_3)_3H$ (s)	1.216	−0.243	−0.176	−0.033	−0.286
$[(CO)_4Mo(\mu\text{-}H)_2Mo(CO)_4]^{2-}$ [1]	1.319	−0.330	−0.609	−0.604	

[a] Without inclusion of 3d AO's of P. [b] With inclusion of 3d AO's of P.

Table 3

Atomic charges and overlap populations for $[(PH_3)_4Mo(\mu\text{-}H)_2Mo(PH_3)_4]^{2+}$ with symmetric and asymmetric bridge calculated by use Fenske–Hall method

Bridge core	M	H^B	$(PH_3)_I$	$(PH_3)_{II}$
Mo(μ-H)₂Mo (symmetric)	0.374	−0.431	0.304	0.230
Mo(μ-H)₂Mo (asymmetric)	0.421	−0.423	0.297	0.233 [a] 0.190 [b]

Bridge core	M—M	M—H$_B$	M—P$_I$	M—P$_{II}$
Mo(μ-H)₂Mo (symmetric)	0.222	0.157	0.239	0.156
Mo(μ-H)₂Mo (asymmetric)	0.193	0.063 [a] 0.256 [b]	0.237	0.154 [a] 0.149 [b]

[a] Position cis to shorter Mo–H$_B$ bond. [b] Position trans to shorter Mo–H^B bond.

and Mo–Mo levels (Fig. 4). As a result of this energy level exchange, the energy level showing M–M interaction becomes the HOMO level. The difference between HOMO and LUMO energy levels increases significantly on going from $[(PH_3)_4Mo(\mu\text{-}H)_2Mo(PH_3)_4]^{2+}$ to $H(PH_3)_3Mo(\mu\text{-}H)_2Mo(PH_3)_3H$ indicating that the stability of the latter complex is higher.

$H(PH_3)_3Mo(\mu\text{-}H)_2Mo(PH_3)_3H$ is the model system for $H(PMe_3)_3Mo(\mu\text{-}H)_2Mo(PMe_3)_3H$ in which asymmetry of the double hydrogen bridge exists. This consideration was included in our calculations but we cannot say which double hydrogen bridge, the symmetric, $Mo(\mu\text{-}H)_2Mo$, or asymmetric, $Mo(\mu\text{-}H)_2Mo$, is the more stable because the energy difference between appropriate levels for both complexes are well within the error margin of the calculations (0.01eV). As one can see from Table 3 the transition from $Mo(\mu\text{-}H)_2Mo$ to $Mo(\mu\text{-}H)_2Mo$ has no significant influence on the charge localized on the bridge hydrogen atoms.

Some similarity between the electronic charge distribution for the bridge core $Mo(\mu\text{-}H)_2Mo$ in $[(CO)_4Mo(\mu\text{-}H)_2Mo(CO)_4]^{2-}$ and $[(PH_3)_4\text{-}$

Table 4
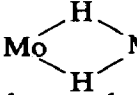
Energies and compositions of the highest occupied molecular energy levels of $[(PH_3)_4Mo\langle{}^H_H\rangle Mo(PH_3)_4]^{2+}$ with symmetric double hydrogen bridge and D_{2h} symmetry calculated by use of the EHT method
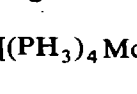
MO	Energy	Greatest contributions by valence atomic orbitals (%)							
$5b_{2g}$	−9.72	$3dP_{II}$	38	$4d_{xz}Mo$	29	sH_{II}	12	pP_{II}	8
$9a_g$	−9.99	$3dP_I$	32	sH_I	10	$3dP_{II}$	8	$4d_{x^2-y^2}Mo$	8
$6b_{1u}$ LUMO	−11.14	$3dP_{II}$	39	sH_{II}	24	$4d_{z^2}Mo$	24	$4d_{x^2-y^2}Mo$	6
$3a_u$ HOMO	−11.38	$4d_{xy}Mo$	31	$4d_{z^2}Mo$	24	$3dP_{II}$	26	$3dP_I$	10
$4b_{1g}$	−11.73	$3dP_I$	32	sH_I	22	$4d_{xy}Mo$	21	sH_{II}	6
$8a_g$	−11.83	$4d_{z^2}Mo$	27	$3dP_{II}$	26	sH_{II}	16	$3dP_I$	8
$4b_{3g}$	−12.18	$3dP_I$	44	sH_I	34	pP_I	13	sP_I	3
$5b_{2u}$	−12.37	$4d_{yz}Mo$	50	$3dP_I$	20	$3dP_{II}$	12	sH_I	8
$3b_{1g}$	−12.58	$3dP_I$	32	$4d_{xy}Mo$	24	sH_I	21	sP_I	6
$5b_{1u}$	−13.92	$4d_{x^2-y^2}Mo$	31	pP_I	26	pP_{II}	19	$4d_{z^2}Mo$	7
$7a_g$	−13.97	sH^B	36	pP_{II}	23	p_zMo	15	$4d_{z^2}Mo$	5
$3b_{3g}$	−14.45	pP_I	45	p_yMo	12	sH_I	6	sH_{II}	5
$5b_{3u}$	−14.76	pP_{II}	35	$4d_{xz}Mo$	27	sH_B	20	sH_{II}	10
$4b_{2g}$	−15.02	pP_{II}	57	sH_I	10	sH_{II}	8	p_xMo	5
$3b_{2g}$	−15.11	pP_{II}	34	sH_{II}	25	pP_I	9	$4d_{xz}Mo$	1
$6a_g$	−15.45	$4d_{x^2-y^2}Mo$	23	pP_{II}	17	pP_I	15	sH_B	12
$4b_{3u}$	−15.54	pP_{II}	34	sH_{II}	20	sH_B	17	$4d_{xz}Mo$	19
$3b_{3u}$	−15.69	pP_{II}	43	sH_B	18	p_xMo	13	sH_{II}	8
$4b_{1u}$	−15.78	pP_{II}	61	sH_{II}	15	pP_I	9	$4d_{z^2}Mo$	5
$2a_u$	−15.80	sP_I	29	sH_I	30	pP_{II}	15	$4d_{x^2-y^2}Mo$	6
$2b_{2g}$	−16.14	pP_I	30	pP_{II}	26	p_xMo	8	$4d_{xz}Mo$	7
$3b_{1u}$	−16.52	pP_{II}	45	sH_{II}	17	pP_I	10	sH_I	10
$4b_{2u}$	−16.77	pP_I	37	pP_{II}	12	sH_I	12	p_yMo	5

Table 5

Energies and compositions of the highest occupied molecular energy levels of $H(PH_3)_3Mo\left\langle\begin{smallmatrix}H\\H\end{smallmatrix}\right\rangle Mo(PH_3)_3H$ with symmetric double hydrogen bridge and C_{2h} symmetry by use of the EHT method
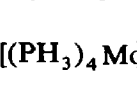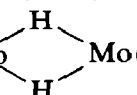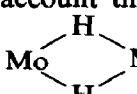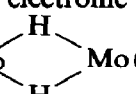
MO	Energy	Greatest contributions by valence atomic orbitals (%)							
$7b_g$	−9.74	$3dP_{II}$	38	$4d_{xz}Mo$	28	pP_{II}	8	sH_{II}	6
$11a_g$	−10.20	$3dP_{II}$	26	$4d_{yz}Mo$	24	$3dP_I$	10	sH^T	9
$10b_u$ LUMO	−11.08	$3dP_{II}$	37	$4d_{z^2}Mo$	24	sH_{II}	17	$4d_{xy}Mo$	8
$7a_u$ HOMO	−11.27	$4d_{xy}Mo$	39	$4d_{z^2}Mo$	17	$3dP_{II}$	17	$3dP_I$	11
$10a_g$	−11.78	$4d_{z^2}Mo$	35	$3dP_{II}$	20	sH_{II}	20	$4d_{xy}Mo$	9
$6b_g$	−11.90	$4d_{xy}Mo$	50	$3dP_I$	16	$3dP_I$	14	sH_{II}	8
$9b_u$	−12.19	$4d_{yz}Mo$	61	$3dP_I$	11	$3dP_{II}$	13	sH_{II}	5
$9a_g$	−13.59	sH^T	39	p_yMo	12	$3dP_I$	11	sH_I	10
$8b_u$	−13.75	sH^T	38	$4d_{x^2-y^2}Mo$	26	$4d_{z^2}Mo$	7	pP_{II}	7
$8a_g$	−14.01	sH^B	33	pP_{II}	30	p_zMo	16	sH^T	4
$6a_u$	−14.74	pP_{II}	28	$4d_{xz}Mo$	28	sH^B	20	sH_{II}	11
$5b_g$	−15.08	pP_{II}	57	sH_{II}	18	p_xMo	3	pP_I	4
$7b_u$	−15.20	pP_{II}	46	pP_I	12	sH^T	10	sH_{II}	7
$7a_g$	−15.22	$4d_{x^2-y^2}Mo$	27	pP_I	25	pP_{II}	15	sH^B	9
$5a_u$	−15.53	pP_{II}	34	sH_{II}	21	$4d_{xz}Mo$	19	sH^B	17
$4b_g$	−15.61	pP_{II}	47	sH_{II}	20	$4d_{xz}Mo$	10	p_xMo	7
$4a_u$	−15.63	pP_{II}	33	sH^B	18	p_xMo	14	sH_I	7
$6b_u$	−15.92	pP_{II}	40	pP_I	23	sH_{II}	14	sH^T	4
$6a_g$	−16.28	pP_{II}	50	sH_{II}	18	sH^B	9	p_zMo	2
$3b_g$	−17.04	pP_I	39	sH_{II}	33	sH^T	11	pP_{II}	9
$3a_u$	−17.10	pP_I	37	sH_I	21	sH_{II}	7	sH^B	2
$5b_u$	−17.13	pP_I	34	pP_{II}	20	sH_I	21	sH_{II}	7

78

$Mo\overset{H}{\underset{H}{<>}}Mo(PH_3)_4]^{2+}$ despite the differing Mo-Mo distances, formal charges on the metal atoms, and terminal ligands in the complexes can be seen in Table 2. The negative charge on bridging hydrogen atom (H^B) and Mo–H^B overlap population in
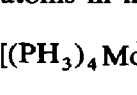
$[(PH_3)_4Mo\overset{H}{\underset{H}{<>}}Mo(PH_3)_4]^{2+}$ are very close to the relevant values in

$[(CO)_4Mo\overset{H}{\underset{H}{<>}}Mo(CO)_4]^{2-}$. By contrast, the positive charge on the molybdenum atom is significantly lower in the carbonyl dimer than in the phosphine dimer because of the differing terminal ligands in the molybdenum dimers. The carbonyl groups accept electronic density from the $4d$ AO's of Mo as reflected in their negative charges, and the phosphine groups donate electronic density to $4d$ AO's of Mo, hence their positive charge.
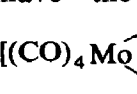
In order elucidate the role of the phosphorous $3d$ AO's in maintaining the Mo–PH_3 bond we calculated by EHT the electronic structures of

$[(PH_3)_4Mo\overset{H}{\underset{H}{<>}}Mo(PH_3)_4]^{2+}$ and $H(PH_3)_3Mo\overset{H}{\underset{H}{<>}}Mo(PH_3)_3H$ taking into account these AO's (Tables 4, 5). The electronic charge distributions for $[(PH_3)_4$

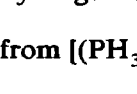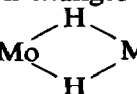$Mo\overset{H}{\underset{H}{<>}}Mo(PH_3)_4]^{2+}$ and $[(CO)_4Mo\overset{H}{\underset{H}{<>}}Mo(CO)_4]^{2-}$ were found to become more similar (Table 6). The positive charge on molybdenum atoms is 1.554 in the phosphine dimer and 1.319 in the carbonyl dimer. The PH_3 groups have the negative charges, as do the CO groups. Thus the PH_3 groups show some acceptor character, which is reflected in the significant participation of $3d$ AO's of the P atoms in maintaining the terminal Mo–PH_3 bonds. The energy level diagrams for

$[(PH_3)_4Mo\overset{H}{\underset{H}{<>}}Mo(PH_3)_4]^{2+}$ calculated by use of the two methods are similar (Fig. 4 and Fig. 6). The AOs of the bridging hydrogen atoms are delocalized and make up five occupied molecular levels. The nonbonding PH_3, and bonding Mo–PH_3 levels which are made up exclusively of the $3p$ AO's of P, lie in the same energy range as the bridge levels. The differences lie in the composition of the highest occupied levels, which have Mo $4d$ AO characters to about 90%, if we disregard the $3d$ AO's of P in the calculations. If the $3d$ P AOs are taken into consideration these levels then correspond to the interactions of the filled $4d$ AO's of Mo atoms with unfilled orbitals of terminal ligands ($4d$ Mo $\rightarrow$ $3d$ P) and therefore have the same character as the highest occupied energy levels in

$[(CO)_4Mo\overset{H}{\underset{H}{<>}}Mo(CO)_4]^{2-}$ ($4d$ Mo $\rightarrow$ π^a CO). It is of interest to note how the electronic charge distribution changes after replacement of the two $(PH_3)_1$ groups with two H^- anions. We have stated that the negative charge on the bridging hydrogen atoms and the Mo–H^B overlap population changes slightly after on going

from $[(PH_3)_4Mo\overset{H}{\underset{H}{<>}}Mo(PH_3)_4]^{2+}$ to $H(PH_3)_3Mo\overset{H}{\underset{H}{<>}}Mo(PH_3)_3H$ (Table 6).

$E\,(eV)$

-10

-15

-20

-25

LUMO $\longrightarrow$
HOMO $\longrightarrow$

$ls H_B$ $\longrightarrow$

$ls H_B$ $\longrightarrow$
$ls H_B$ $\longrightarrow$

$ls H_B$ $\longrightarrow$
$ls H_B$ $\longrightarrow$

$ls H_B$ $\longrightarrow$

$ls H_B$ $\longrightarrow$

$5b_{3g}$

$6b_{1a}$ — — — — LUMO
$4b_{1g}$
$4b_{3g}$
$3a_u$ — — — — HOMO

$3b_{1g}$

$5b_{2u}$

$8a_g$

$ls H_T$
$ls H_T$

$7a_g$
$5b_{3u}$

$5b_{1u}$, $3b_{3g}$, $4b_{2g}$

$6a_g$
$4b_{3u}$

$4b_{2u}$, $5a_g$, $3b_{1u}$, $4b_{1u}$, $3b_{2g}$

$3b_{3u}$
$2b_{2g}$, $2a_u$

$4a_g$

$11a_g$

$10b_u$

$7a_u$

$9a_g$
$8b_u$
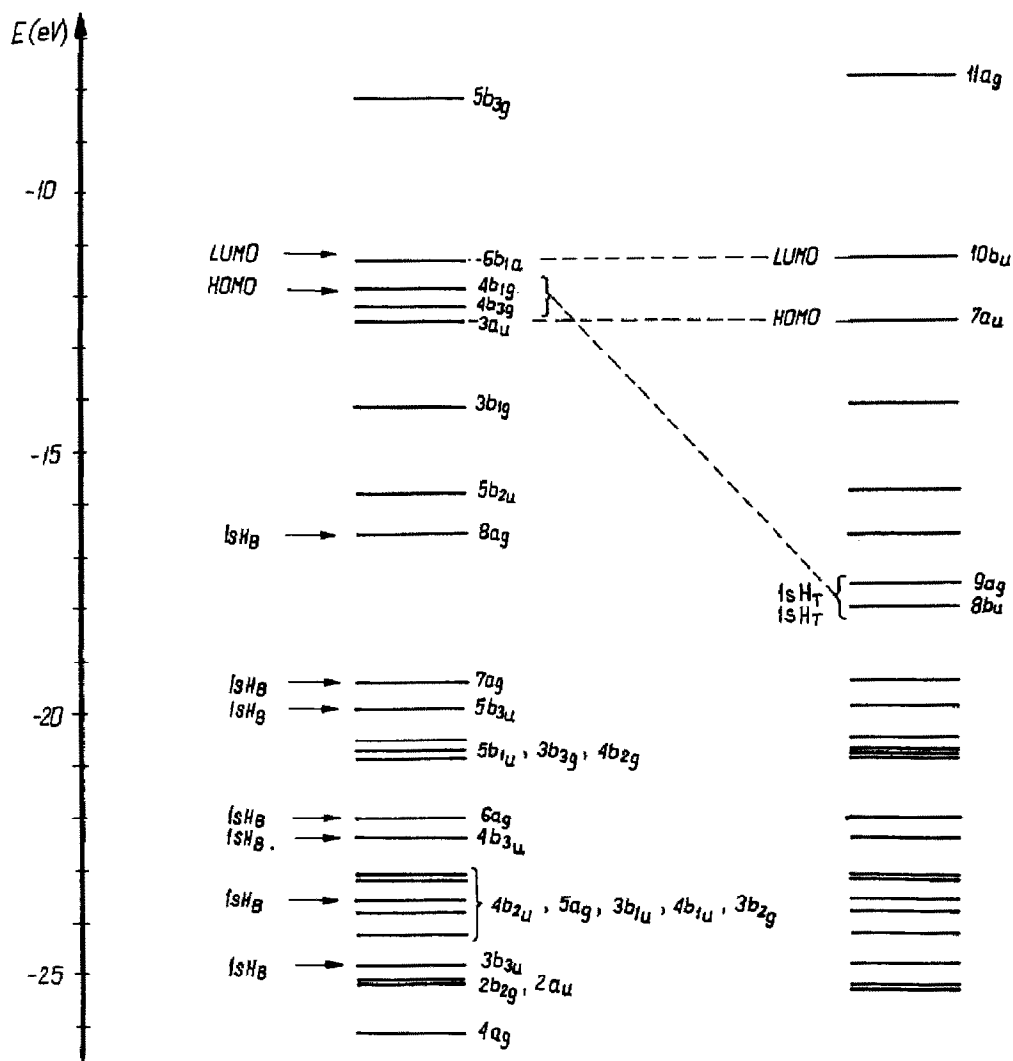
Fig. 6. Correlation of the molecular energy levels of $[(PH_3)_4 Mo \diagdown ^H \diagdown ^H Mo(PH_3)_4]^{2+}$ and $H(PH_3)_3 Mo \diagdown ^H \diagdown ^H Mo(PH_3)_3 H$ calculated by use of the EHT method.

However, the changes of the charge on metal atoms and PH_3 groups are larger. The positive charge on the metal atoms decreases from 1.554 to 1.216 and the negative charge on the PH_3 groups increases from -0.123 to -0.176 for $(PH_3)_I$ and increase from -0.037 to -0.333 for $(PH_3)_{II}$. Thus the electronic density was partially shifted from the terminal H^- anions via the $4d$ metal atom AO's onto the $3d$ AO's of the P atoms. The Mo–PH_3 overlap population is also slightly increased. These two facts indicate that the Mo–PH_3 bonds are stronger in $H(PH_3)_3 Mo \diagdown ^H \diagdown ^H Mo(PH_3)_3 H$ than in $[(PH_3)_4 Mo \diagdown ^H \diagdown ^H Mo(PH_3)_4]^{2+}$. A char-
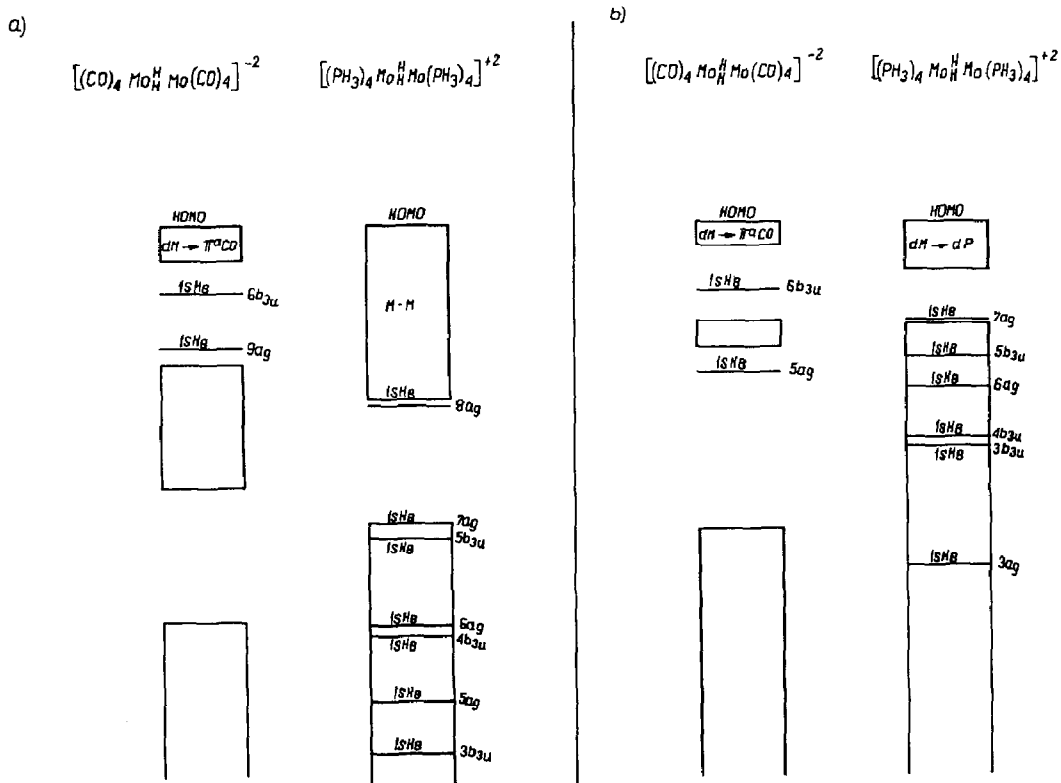
Fig. 7. Comparison of the electronic structure of the carbonyl and phosphine dimers of Mo with double hydrogen bridge: a) on the basis of the calculations by use of the Fenske–Hall method b) on the basis of the calculations by use of the EHT method.

acteristic feature of the Mo–H–Mo bridge bond in all complexes of molybdenum studied by us up to now is its partial ionic character.

The terminal Mo–H bond has the same character as the Mo–H–Mo bridge bond in H(PH$_3$)$_3$Mo⟨$_H^H$⟩Mo(PH$_3$)$_3$H because of the negative charge on the terminal hydrogen atom. This negative charge is -0.286 compared with -0.246 for the bridge hydrogen atom. The covalencies of the Mo–H and Mo–H–Mo bonds are also similar, because the Mo–H overlap population for terminal hydrogen atoms (0.404) is only slightly higher than the Mo–H overlap population for the bridge hydrogen atoms (0.363).

However, the energy levels corresponding to the terminal Mo–H bonds are higher than all the levels corresponding to the Mo–H–Mo bonds and thus the terminal hydrogen bonds are less stable than the bridge hydrogen bonds in this molecule (Fig. 4 and Fig. 6).

In Fig. 7 is depicted the comparison of the energy levels of [(CO)$_4$Mo⟨$_H^H$⟩Mo(CO)$_4$]$^{2-}$ and [(PH$_3$)$_4$Mo⟨$_H^H$⟩Mo(PH$_3$)$_4$]$^{2+}$ which were

calculated by use of the Fenske–Hall and EHT methods. As mentioned in a previous paper, the stability of the double hydrogen bridge is higher in the phosphine dimer of Mo than in its carbonyl dimer [2]. It is noteworthy that the stabilities of the double hydrogen bridges in the phosphine dimer of Mo and in

$(CH_3)_4Al$ ⟨H over H bridge⟩ $Al(CH_3)_4$ are similar. On the other hand the stability of the

double hydrogen bridge in carbonyl dimers of the transition metals is similar to that

in ⟨H₂B(H₂)BH₂ diborane-type bridge structure⟩ .
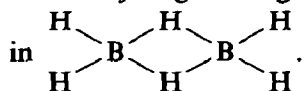
Conclusions

We have found that the Mo–H–Mo bridge bond in the phosphine binuclear complex of molybdenum, like that in the carbonyl dimer of molybdenum, is partly ionic and partly covalent. The Mulliken negative charge on bridging hydrogen atom is in a range of values characteristic for other complexes of molybdenum which we have studied previously [1,5,6]. The highest filled energy levels in this complex correspond to the interactions of the filled 4d AO's of the metal atoms with the unfilled 3d AO's of the phosphine atoms, so in this respect the electronic structure of the phosphine dimer also reflects the electronic structure of the carbonyl dimer too. On the other hand the stability of the double hydrogen bridge and the delocalization of the molecular orbitals corresponding to the M–H–M bonds are much higher in the phosphine complex. The effective bonding interaction between metal atoms corresponds to a direct M–M bond of order slightly higher than two. We have also mentioned that in the $H(PH_3)_3Mo$ ⟨H over H bridge⟩ $Mo(PH_3)_3H$ the terminal hydrogen ligands have a similar negative charge to that of the bridge hydrogen ligands, so that the Mo–H and the Mo–H–Mo bonds have partial ionic character. But the stability of the Mo–H–Mo bridge bonds is higher than that of the terminal Mo–H bonds.

Acknowledgement

References

1 B. Jeżowska-Trzebiatowska and B. Nissen-Sobocińska, J. Organomet. Chem., 342 (1988) 215.
2 R.A. Jones, K.W. Chiu, G. Wilkinson, A.M.R. Galas, M.B. Hursthay, J.Chem. Soc. Chem. Comm., (1980) 408.
3 M.B. Hall and R.F. Fenske, Inorg. Chem., 11 (1972) 768.
4 R. Hoffmann, J. Chem. Phys., 39 (1963) 1397.
5 B. Jeżowska-Trzebiatowska and B. Nissen-Sobocińska, J. Organomet. Chem., 322 (1987) 331.
6 B. Jeżowska-Trzebiatowska and B. Nissen-Sobocińska, J. Organomet. Chem., 342 (1988) 353.